ANALYZING SPECTRAL REGROWTH OF QPSK AND OQPSK SIGNALS

Raviv Raich and G. Tong Zhou

School of Electrical and Computer Engineering, Georgia Institute of technology, Atlanta, GA 30332-0250
raviv, gtz@ece.gatech.edu

ABSTRACT

In this paper, a comparison is made between the spectral regrowth of quadrature phase shift keyed (QPSK) and offset QPSK (OQPSK) signals as they go through non-linear amplifications. Contrary to existing approaches that assume the power amplifier input is Gaussian, our analysis is carried out without the Gaussian assumption, by using higher-order statistics. We show that it is possible to assess quantitatively, whether and how much OQPSK is beneficial in reducing spectral regrowth. Simple closed form formulas are obtained when the pulse shape filter is time-limited. A particular measure of spectral broadening is also provided.

1. INTRODUCTION

QPSK is a popular modulation format that is used in many applications (e.g., IS-95 CDMA). Let us denote a QPSK symbol by s_m where $s_m = [\pm 1 \pm j]$ with probability 0.25 each. A significant drawback of QPSK is the ± 180-degree phase change at the $1+j \leftrightarrow -1-j$ and the $1-j \leftrightarrow -1+j$ transitions. Such transitions are undesirable if the waveform is to be filtered and subsequently processed by a nonlinear power amplifier (PA).

Nonlinear PAs are used in communication systems for improved efficiency because generally, there is an inverse relationship between linearity and efficiency [1]. Higher efficiency means that a larger percentage of the dc (e.g., battery) power is delivered to the load, thus increasing battery life and minimizing heat dissipation.

Figure 1 shows in solid line, the AM/AM (amplitude to amplitude) conversion of a nonlinear PA. The dashed line shows in comparison, a linear AM/AM response. Although $|s_m| = \sqrt{2}$ is constant modulus, the envelope of a filtered QPSK signal could fluctuate, thus leading to nonlinear distortions. In Figure 1, this means that a filtered QPSK signal could traverse the A-C region of the PA response. In addition to the PA compression at the larger amplitudes, the filtered QPSK signal also experiences cut-off when the input amplitude is close to zero.

A remedy is to employ offset QPSK (OQPSK) modulation. In OQPSK, the I- and Q- symbol streams are offset in time by half the symbol period, thus avoiding the ± 180-degree phase change. For illustration purpose, we can imagine that in Figure 1, instead of the A-C region, the filtered OQPSK signal traverses through the B-C region of the PA, thus avoiding cut-off.

Despite of this merit of OQPSK, some concerns were raised about the overall effectiveness of employing OQPSK. First of all, it does not lend itself to differential encoding [2]. Furthermore, argument has been made that although the QPSK signal experiences the cut-off effect, it spends a very small percentage of time in the cut-off region. On the other hand, the region that the OQPSK signal spends its time with (e.g., the B-C region in Figure 1) is more compressed and hence more nonlinear than the A-B region that the QPSK signal frequently visits.

This work was supported in part by the National Science Foundation grant MIP 9703312 and by the State of Georgia's Yamacraw Initiative.

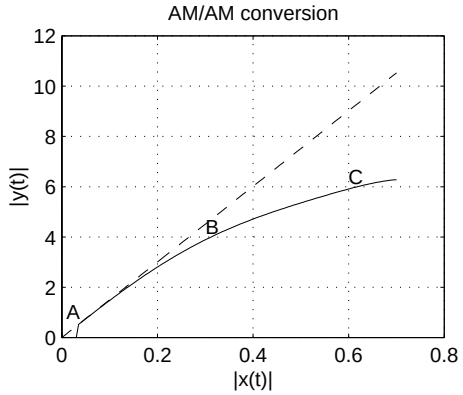

Fig. 1. AM/AM characteristic of a nonlinear PA (solid line).

This paper attempts to offer a means of quantitatively analyzing spectral regrowth of a communication signal passing through a nonlinear device. Specifically, we compare the power spectra of filtered QPSK and OQPSK signals after their nonlinear amplification. Although spectral analysis is routinely carried out for communications signals, the nonlinearity present in the PA complicates the problem. In [3], the authors analyzed the spectral regrowth pattern when the input signal is Gaussian, but their results have limited applicability since many communication signals are non-Gaussian. In [4], a Volterra system approach was adopted. We address here spectral regrowth of a memoryless nonlinear device.

2. PROBLEM FORMULATION

A linearly modulated signal is expressed in the baseband as

$$x(t) = \frac{A}{\sqrt{2}} \sum_{m=-\infty}^{\infty} s_m \, h\left(t - mT\right), \tag{1}$$

where $s_m = a_m + jb_m$ is the mth symbol transmitted, $h(t)$ is the baseband pulse shape filter, A is a real-valued input scale factor, and T is the symbol period. We assume that a_m and b_m are *i.i.d.* and are mutually independent. We refer to the resulting s_m as circular complex symmetric.

When s_m is QPSK, we have $a_m \in \{1, -1\}$ with equal probability 0.5, and similarly for b_m.

A filtered OQPSK signal may be written as:

$$\begin{aligned} x(t) &= \frac{A}{\sqrt{2}} \sum_{m=-\infty}^{\infty} a_m h\left(t - mT\right) \\ &\quad + j\,\frac{A}{\sqrt{2}} \sum_{m=-\infty}^{\infty} b_m h\left(t - mT - \frac{T}{2}\right), \end{aligned} \tag{2}$$

where a_m, b_m, $h(t)$, A, and T are the same as in the filtered QPSK case. The only difference is that the imaginary part of (2) has a $T/2$ delay relative to that of (1).

Next, $x(t)$ is input to a PA to yield output $y(t)$. Ideally, we would like $y(t) = \alpha\, x(t)$, where α is a constant with $|\alpha| > 1$. But in reality, all PAs are inherently nonlinear. In the case of a memoryless nonlinear PA, we can approximate its baseband input/output relationship by [5, p. 735]:

$$y(t) = x(t) \sum_{n=0}^{\infty} a_{2n+1}\, |x(t)|^{2n}, \tag{3}$$

from which we infer that the complex gain is

$$\frac{y(t)}{x(t)} = \sum_{n=0}^{\infty} a_{2n+1}\, |x(t)|^{2n}. \tag{4}$$

It is seen that the complex gain is a function of the input amplitude $|x(t)|$ only. This is consistent with the fact that a memoryless nonlinear PA is often characterized by its AM/AM (i.e., $|y(t)|$ vs. $|x(t)|$) and AM/PM (i.e., $\angle y(t) - \angle x(t)$ vs. $|x(t)|$) characteristics. If $|x(t)|$ is constant such as the case of (1) with a rectangular shaped $h(t)$ (see also Section 3), then $x(t)$ will not experience any nonlinear distortion since the gain in (4) is constant. Our objective here is to analyze the power spectral density (PSD) of $y(t)$ and its dependence on the PA parameters $\{a_{2n+1}\}$, the baseband filter $h(t)$, and the input scale factor A.

3. ANALYSIS

Although our analysis on spectral regrowth can be generalized to accommodate higher-order nonlinearities, for simplicity, we illustrate our approach using a 3rd-order nonlinear model:

$$\begin{aligned} y(t) &= a_1 x(t) + a_3\, |x(t)|^2 x(t) \\ &= a_1 x(t) + a_3\, x^2(t) x^*(t). \end{aligned} \tag{5}$$

Since s_m has a symmetric distribution, $y(t)$ has zero-mean. Therefore, the auto-correlation and auto-covariance functions of $y(t)$ coincide. We define the auto-correlation function of $y(t)$ at time t and lag τ as follows:

$$c_{2y}(t; \tau^*) = E[y(t)\, y^*(t+\tau)]. \tag{6}$$

In (6), τ^* indicates that conjugation is applied to the lagged copy, $y(t+\tau)$. Note that τ itself is always a real number.

Since $y(t)$ is cyclostationary, its time-averaged auto-correlation function is

$$\bar{c}_{2y}(\tau) = \frac{1}{T} \int_0^T c_{2y}(t; \tau^*)\, dt. \tag{7}$$

The power spectrum of $y(t)$ is the Fourier transform of $\bar{c}_{2y}(\tau)$:

$$\begin{aligned} S_{2y}(f) &= \mathcal{F}_{\tau \to f} \left\{ \bar{c}_{2y}(\tau) \right\} \\ &= \int_{-\infty}^{\infty} \bar{c}_{2y}(\tau)\, e^{-j2\pi\tau f}\, d\tau. \end{aligned} \tag{8}$$

We would like to examine $S_{2y}(f)$ for the PA model in (5) and the input as in (1) or (2). Substituting (5) into (6), we obtain

$$\begin{aligned} c_{2y}(t;\tau) &= E\left[y(t) y^*(t+\tau)\right] \\ &= |a_1|^2 E\left[x(t) x^*(t+\tau)\right] \\ &\quad + a_1 a_3^* E\left[x(t) |x(t+\tau)|^2 x^*(t+\tau)\right] \\ &\quad + a_3 a_1^* E\left[x^*(t+\tau) |x(t)|^2 x(t)\right] \\ &\quad + |a_3|^2 E\left[|x(t)|^2 x(t) |x(t+\tau)|^2 x^*(t+\tau)\right]. \end{aligned} \tag{9}$$

Alternatively, we write

$$\begin{aligned} c_{2y}(t;\tau) &= |a_1|^2\, \phi_{11}(t;\tau) + a_1 a_3^*\, \phi_{13}(t;\tau) \\ &\quad + a_3 a_1^*\, \phi_{31}(t;\tau) + |a_3|^2\, \phi_{33}(t;\tau) \end{aligned} \tag{10}$$

where

$$\begin{aligned} \phi_{11}(t;\tau) &= \mathrm{cov}\left\{x(t), x^*(t+\tau)\right\} \\ \phi_{13}(t;\tau) &= \mathrm{cov}\left\{x(t)|x(t+\tau)|^2, x^*(t+\tau)\right\} \\ \phi_{31}(t;\tau) &= \mathrm{cov}\left\{x^*(t+\tau), |x(t)|^2 x(t)\right\} \\ \phi_{33}(t;\tau) &= \mathrm{cov}\left\{|x(t)|^2 x(t), |x(t+\tau)|^2 x^*(t+\tau)\right\} \end{aligned} \tag{11}$$

Our next step is to expand the above covariance terms using the Leonov-Shiryaev formula [6]. Under the circular symmetry assumption of s_m, we infer that $x(t)$ of (1) is circular symmetric as well. Therefore, we find for filtered QPSK,

$$\begin{aligned} \phi_{11}(t;\tau) &= c_{2x}(t;\tau^*) \\ \phi_{13}(t;\tau) &= c_{4x}(t;\tau^*,\tau,\tau^*) + 2c_{2x}(t;\tau^*) c_{2x}(t+\tau^*;0) \\ \phi_{31}(t;\tau) &= c_{4x}(t;0^*,0,\tau^*) + 2c_{2x}(t;\tau^*) c_{2x}(t;0^*) \\ \phi_{33}(t;\tau) &= c_{6x}(t;0^*,0,\tau^*,\tau,\tau^*) \\ &\quad + 4c_{4x}(t;0^*,\tau,\tau^*) c_{2x}(t;\tau^*) \\ &\quad + 2c_{4x}(t;\tau^*,\tau,\tau^*) c_{2x}(t;0^*) \\ &\quad + 2c_{4x}(t;0^*,0,\tau^*) c_{2x}(t+\tau;0^*) \\ &\quad + c_{4x}(t;0,\tau^*,\tau^*) c_{2x}(t^*;\tau) \\ &\quad + 4c_{2x}(t;\tau^*) c_{2x}(t;0^*) c_{2x}(t+\tau;0^*) \\ &\quad + 2c_{2x}(t;\tau^*) c_{2x}(t;\tau^*) c_{2x}(t^*;\tau). \end{aligned}$$

Note that the OQPSK signal (2) is no longer circular symmetric and hence the corresponding ϕ_{13}, ϕ_{31}, and ϕ_{33} expressions contain additional terms.

The kth-order cumulant of $x(t)$ at time t and lags $(\tau_1, \ldots, \tau_{k-1})$ is defined as

$$\begin{aligned} & c_{kx}(t;\tau_1,\ldots,\tau_{\ell-1},\tau_\ell^*,\ldots,\tau_{k-1}^*) \\ \triangleq\ & \mathrm{cum}\{x(t), x(t+\tau_1), \ldots, x(t+\tau_{\ell-1}), \\ & \qquad x^*(t+\tau_\ell), \ldots, x^*(t+\tau_{k-1})\}. \end{aligned}$$

Note that a conjugated lag in the argument of $c_{kx}(\cdot)$; e.g., τ_ℓ^*, implies that the corresponding term in the cumulant; e.g., $x^*(t+\tau_\ell)$, has conjugation. For the $x(t)$ in (1), we have

$$\begin{aligned} & c_{kx}(t;\tau_1,\ldots,\tau_\ell^*,\ldots,\tau_{k-1}^*) \\ =\ & \gamma_{ks} \left(\frac{A}{\sqrt{2}}\right)^k \sum_m h(t-mT) h(t-mT+\tau_1) \ldots \\ & h(t-mT+\tau_{\ell-1}) h^*(t-mT+\tau_\ell) \ldots h^*(t-mT+\tau_{k-1}), \end{aligned}$$

and

$$\gamma_{ks} = \mathrm{cum}\left\{s(t), s(t+\tau_1), \ldots, s(t+\tau_{\ell-1}),\right.$$

$$s^*(t+\tau_\ell), \ldots, s^*(t+\tau_{k-1})\}.$$

Next, let us analyze $S_{k\ell}(f)$, which is the Fourier transform of $\bar{\phi}_{k\ell}(\tau)$, the time-average of $\phi_{k\ell}(t;\tau)$.

Interestingly, when $h(t) = 0, \forall\ |t| > T/2$, the $\phi_{k\ell}(t;\tau)$ expressions can be simplified considerably. As a result, we obtain

$$S_{11}(f) = \frac{A^2}{T}|H(-f)|^2 \quad (12)$$

$$S_{13}(f) = \frac{A^4}{T}H(-f)\left[H(f) \circledast H^*(-f) \circledast H^*(-f)\right] \quad (13)$$

$$S_{31}(f) = \frac{A^4}{T}H^*(-f)\left[H^*(f) \circledast H(-f) \circledast H(-f)\right] \quad (14)$$

$$S_{33}(f) = \frac{A^6}{T}\left|H^*(f) \circledast H(-f) \circledast H(-f)\right|^2, \quad (15)$$

where $H(f)$ is the Fourier transform of $h(t)$, and $\circledast$ is the convolution operator.

When $h(t)$ is real valued and symmetric, we obtain a surprisingly simple expression for the PSD of $y(t)$:

$$S_{2y}(f) = |a_1|^2 A^2 \frac{1}{T}\left|H(f) + \frac{a_3}{a_1}A^2 H_3(f)\right|^2 \quad (16)$$

where $H_3(f) = H(f) \circledast H(f) \circledast H(f)$.

We make the following remarks regarding (16):

Remark 1: Potential spectral regrowth is indicated by the $H_3(f)$ term which generally expands the bandwidth of $H(f)$ through the triple convolution.

Remark 2: The severity of spectral regrowth is determined by the coefficient $(a_3/a_1)A^2$ in (16). If the PA is inherently very nonlinear; i.e., the a_3/a_1 ratio is high, then one needs to reduce the input amplitude factor A in order to minimize spectral regrowth – this is referred to as input back-off. In general, spectral regrowth becomes more severe as A increases.

Now let us consider two baseband filters often studied in the literature [7]:

$$h(t) = \begin{cases} 1 & |t| \le \frac{T}{2} \\ 0 & |t| > \frac{T}{2} \end{cases} \quad (17)$$

and

$$h(t) = \begin{cases} \sqrt{2}\cos(\pi\frac{t}{T}) & |t| \le \frac{T}{2} \\ 0 & |t| > \frac{T}{2}. \end{cases} \quad (18)$$

For the rectangular pulse (17), we obtain

$$H(f) = \frac{1}{f_o}\frac{\sin(\frac{f\pi}{f_o})}{(\frac{f\pi}{f_o})}, \quad (19)$$

and

$$H_3(f) = \frac{1}{f_o}\frac{\sin(\frac{f\pi}{f_o})}{(\frac{f\pi}{f_o})} = H(f). \quad (20)$$

Substituting (19)-(20) into (16), we infer that there is no spectral regrowth when the rectangular pulse is used for the $x(t)$ in (1). This is expected since in this case, the resulting $|x(t)| = A$ has constant envelope.

For the sinusoidal pulse (18), we have

$$H(f) = \frac{\sqrt{2}}{2\pi f_o}\frac{\cos(\frac{f\pi}{f_o})}{\frac{1}{4} - \left(\frac{f}{f_o}\right)^2}, \quad (21)$$

and

$$H_3(f) = \frac{3\sqrt{2}}{2\pi f_o}\frac{\cos(\frac{f\pi}{f_o})}{\left(\frac{1}{4} - \left(\frac{f}{f_o}\right)^2\right)\left(\frac{9}{4} - \left(\frac{f}{f_o}\right)^2\right)}. \quad (22)$$

This $H_3(f)$ can be shown to have a wider mainlobe than $H(f)$.

One way to quantify spectral regrowth is to use a notion of bandwidth $\sqrt{\langle f^2\rangle}$ where

$$\langle f^2\rangle \triangleq \frac{\int_{-\infty}^{\infty}(f - \langle f\rangle)^2 S(f)df}{\int_{-\infty}^{\infty} S(f)df} \quad (23)$$

and

$$\langle f\rangle \triangleq \frac{\int_{-\infty}^{\infty} f S(f)df}{\int_{-\infty}^{\infty} S(f)df}. \quad (24)$$

Note that for a symmetric spectrum $S(f)$, the corresponding $\langle f\rangle = 0$.

Substitution of (16), (21), and (22) into (23) yields the following bandwidth formula for the cosine pulse (18):

$$\sqrt{\langle f^2\rangle} = \frac{f_o}{2}\sqrt{\frac{1 - 3\ \mathrm{Re}(\beta) + 4.5\ |\beta|^2}{1 - 3\ \mathrm{Re}(\beta) + 2.5\ |\beta|^2}},$$
$$\beta = -\frac{a_3}{a_1}A^2. \quad (25)$$

When the PA is linear, we have $a_3 = 0$ and hence $\beta = 0$. The bandwidth formula (25) yields $0.5f_o$ as the bandwidth of a linear system. Therefore the ratio, $\sqrt{\langle f^2\rangle}/(0.5f_0)$, can be used as a measure of bandwidth expansion and from (25), it is obvious that this ratio is > 1 for any $\beta \neq 0$.

When $x(t)$ is OQPSK, the analysis is generally more involved. But with either (17) or (18), the OQPSK signal in (2) has $|x(t)| = A$ and hence the corresponding PA output $y(t) = (a_1 + a_3 A^2)x(t)$ does not experience any spectral regrowth.

4. SIMULATIONS

In this section, we present a numerical example to verify the accuracy of the expressions (12)-(16). $1,000$ symbols s_m were generated and a filtered QPSK signal $x(t)$ was obtained from equation (1) with the cosine pulse (18). The scale factor was $A = 1$ and the sampling period was $\frac{1}{40}T$ seconds. The resulting $x(t)$ went through nonlinear amplification as described by (5) with $a_1 = 1$ and $a_3 = -0.3\exp(j\frac{\pi}{4})$.

Figure 2 shows the theoretical $S_{11}(f)$ (c.f. (12)) in solid line and its estimate in dashed line. The estimate is nothing but the PSD estimate of $x(t)$. Close agreement between the two is observed.

Figure 3 shows the theoretical $S_{33}(f)$ (c.f. (15)) in solid line and its estimate – the PSD estimate of $x(t)^2x^*(t)$ in dashed line. Similar agreement is observed. Comparing with Figure 2, we see that the bandwidth of $S_{33}(f)$ has increased from that of $S_{11}(f)$.

Indeed, $\sqrt{\langle f^2 \rangle}$ of $S_{33}(f)$ is $\sqrt{1.8}$ times or 34% larger than that of $S_{11}(f)$ (c.f. (23)). Moreover, evaluation of the (12)-(15) terms reveals that $S_{33}(f)$ is the major contributor to spectral regrowth in $S_{2y}(f)$.

In Figure 4, we show a comparison between the output spectrum $S_{2y}(f)$ when the input is QPSK (solid line) or OQPSK (dashed line). The bandwidth of the QPSK signal is indeed larger than that of the OQPSK signal. In fact, equation (25) with $\beta = 0.3 \exp(j\frac{\pi}{4})$ tells that the bandwidth increase was 14%.

5. CONCLUSIONS

We have described in this paper, an analytical approach for evaluating the power spectra of filtered QPSK and OQPSK signals after nonlinear amplification. A salient feature of our analysis is that we do not need to assume that the PA input is Gaussian. In the QPSK case, we were able to obtain a simple closed form expression for the output PSD when the PA is cubic nonlinear and the baseband filter is time-limited. We treated the cosine pulse filtered QPSK/OQPSK signals in detail and provided a measure of bandwidth expansion. We are currently working on applying our analysis to more general scenarios.

6. REFERENCES

[1] S. C. Cripps, *RF Power Amplifiers for Wireless Communications*, Artech House, Norwood, MA, 1999.

[2] Y. Akaiwa and Y. Nagata, "Highly efficient digital mobile communication with a linear modulation method," *IEEE J. of Selected Areas in Communications*, vol. 5, pp. 890–895, June 1987.

[3] K. G. Gard, H. M. Gutierrez, and M.B. Steer, "Characterization of spectral regrowth in microwave amplifiers based on the nonlinear transformation of a complex gaussian process," *IEEE Trans. on Microwave Theory and Techniques*, vol. 47, no. 7, pp. 1059–1069, July 1999.

[4] A. Gusmão, V. Gonçalves, and N. Esteves, "A novel approach to modeling of OQPSK-type digital transmission over nonlinear radio channels," *IEEE Journal on Selected Areas in Communications*, vol. 15, no. 4, pp. 647–655, May 1997.

[5] S. Benedetto and E. Biglieri, *Principles of Digital Transmission with Wireless Applications*, Kluwer Academic / Plenum Publishers, New York, 1999.

[6] D. R. Brillinger, *Time Series: Data Analysis and Theory*, Holden-day Inc., San Francisco, 1981.

[7] J. G. Proakis, *Digital Communications*, McGraw-Hill, 3rd edition, 1995.

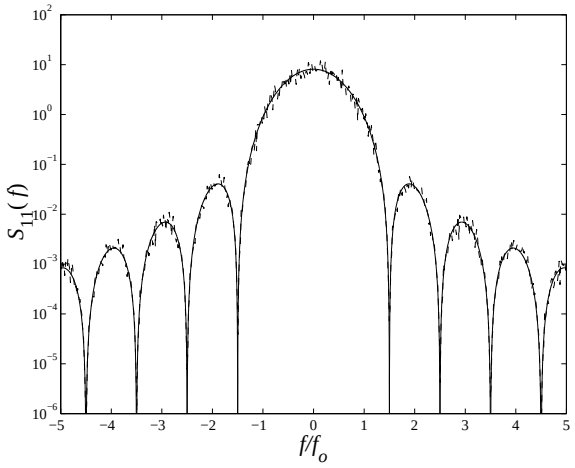

Fig. 2. The theoretical $S_{11}(f)$ (solid line) and its estimate (dashed line).

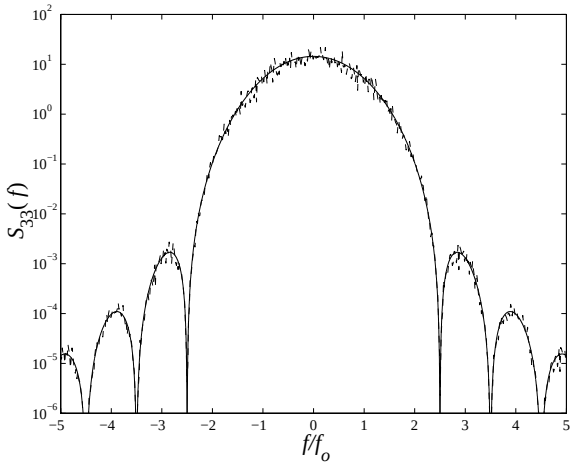

Fig. 3. The theoretical $S_{33}(f)$ (solid line) and its estimate (dashed line).

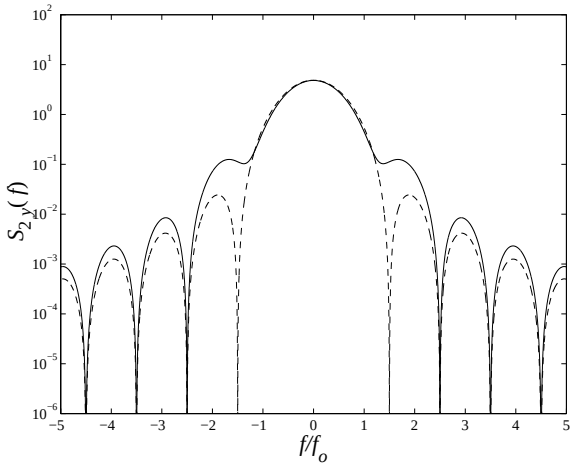

Fig. 4. The PA output PSD $S_{2y}(f)$ when the input is QPSK (solid line) or OQPSK (dashed line).